

Stochastic Models of Neuronal Growth

Cristian Staii*

* Department of Physics and Astronomy, Tufts University, Medford, Massachusetts 02155, USA

*E-mail: Cristian.Staii@tufts.edu

Keywords: Neuron, Axonal Growth, Fokker-Planck Equation, Nonlinear Dynamics, Stochastic Process, Cellular Mechanics

Abstract

Neurons are the basic cells of the nervous system. During their growth neurons extend two types of processes: axons and dendrites, which navigate to other neurons and form complex neuronal networks that transmit electrical signals throughout the body. The basic process underlying the network formation is axonal growth, a process involving the extension of axons from the cell body towards target neurons. During growth axons sense their environment, process information, and respond to external stimuli by adapting their growth dynamics. Environmental stimuli include intercellular interactions, biochemical cues, and the mechanical and geometrical features of the growth substrate. Axonal dynamics is controlled both by deterministic components (tendency to grow in certain preferred directions imparted by surface mechanical and geometrical properties), and a random deviation from these growth directions due to stochastic processes. Several types of stochastic processes are involved in the growth cone dynamics including: intercellular signaling, detection of biomolecules at very small concentrations, biochemical reactions taking place in the growth cone, signal transduction, formation of lamellipodia and filopodia, and the polymerization of actin filaments and microtubules that steer the growth cone. Despite recent impressive advances in our understanding of how neurons grow and form functional connections, a fully quantitative description of axonal dynamics is still missing. In this paper, we present a review of our work on a certain class of stochastic models. We show that Langevin and Fokker-Planck stochastic differential equations provide a powerful theoretical framework for describing how collective axonal dynamics and the formation of neuronal network emerge from biophysics of single neurons and their interactions. We combine this theoretical analysis with experimental data to extract key parameters of axonal growth: diffusion (cell motility) coefficients, speed and angular distributions, mean square displacements, as well as mechanical parameters describing the cell-substrate coupling. These results have important implications for our understanding of fundamental mechanisms involved in neuronal growth and the formation of functional neuronal networks, as well as for bioengineering novel scaffolds and neuroprosthetic devices to promote nerve regeneration.

1. Introduction

Neurons are the basic working units of the brain and are responsible for transmitting electrical and chemical signals throughout the nervous system. During the development of the brain neurons extend (grow) axons actively navigate over distances of the order of 10-100 cell diameters in length to find target dendrites from other neurons and to form neuronal circuits. A key challenge in biological physics is to find the fundamental physical principles that govern axonal dynamics, and in particular to explain the complex architecture of neuronal circuits in terms of a small number of variables. Axonal motion is guided by the growth cone, a dynamic sensing unit located at the leading edge of the axon (**Fig. 1**). The growth cones consistently follow specific pathways through a complex and changing environment by responding to multiple environmental guidance stimuli such as surface-bound extracellular matrix proteins (ECM), biomolecules released by neighboring neurons, electrical signals, substrate stiffness and geometrical cues [1-5].

Over the past decade, there has been rapid progress in our understanding of the role played by chemical signaling and surface-based biochemical guidance on the growth cone dynamics and axonal elongation. For example, it is known that axonal navigation to their target depends on the spatial arrangement of extracellular proteins on the growth surfaces, and that mechanical interactions and physical stimuli play a key role in many of the growth processes [6-16]. It is also known that surface-bound biochemical cues (*e.g.*, netrins, ephrins, semaphorins) can either attract or repel a growth cone [3-7], and that many different types of signal transduction pathways link the activation of growth cone sensors to changes in the internal dynamics of the cytoskeleton [1-3, 6, 7]. While chemical guidance cues are relatively well understood, there is recent evidence showing that physical stimuli present in the extracellular environment (external forces, electric fields, as well as substrate physical properties such as stiffness and geometry) play a very important role during axonal growth and development [8-17].

Much of the research into how external cues influence neuronal growth was performed by studying neuronal growth on substrates *in vitro* where the external stimuli can be controlled [3-5, 18-27]. This previous work demonstrated that mechanical and geometrical cues play a crucial role in axonal growth and the formation of functional connections between neuronal cells. Researchers have used surface patterning to change the physical landscape through which the growth cone navigates and also to direct cellular behavior. For example, it has been shown that altering the substrate stiffness could have dramatic effects on the axonal outgrowth for several types of neurons [10, 15, 16]. Axonal growth has also been studied on microfluidic channels and 3-dimensional constructs of various sizes [18, 19], surfaces with different geometrical features such as symmetric ridges and indentations [21-24], parallel lines and gaps or adhesive micro-lines of various geometries [25-27]. These studies have shown that periodic geometrical features on surfaces increase total axonal outgrowth and tend to bias growth along certain preferred directions, and that the preferred growth orientation with respect to repeating patterns depends on the cell type. However, the fundamental mechanisms that control the cellular responses to external mechanical and geometrical stimuli are not completely understood. In particular there are many key unanswered questions about the mechanisms that control neuron biomechanical response, about the details of cell-substrate interactions such as the synergy or antagonism between various external cues, and about how these interactions affect the formation and function of neuronal networks. Moreover, a comprehensive theoretical model of neuronal growth that includes the relationship between the dynamics of intracellular components, biomechanical properties of single

cells and the collective behavior of axonal dynamics remains elusive. The lack of such knowledge is an important problem, because these stimuli together control the wiring of neural networks *in vivo* and neuronal function from development to homeostasis and to damage/loss of function. To address these questions, we need novel experimental techniques to measure cell-cell and cell-substrate interactions with very high spatial and temporal resolutions, as well as novel theoretical methods that connect cellular dynamics at different scales.

2. Theoretical models of neuronal growth

There is a rich literature dedicated to modeling neuronal growth. Early work focused on interpreting observed neuronal growth using random walk models. For example, Katz and collaborators [28] showed that axonal elongation and retraction was well described by an uncorrelated random walk. Odde and collaborators, however, demonstrated that axonal extension is correlated with a subsequent retraction on time scales of a few minutes [29]. A similar approach was adopted by Buettner and collaborators [30], who extracted probabilistic rules for filopodial dynamics from time-lapse images and formalized these as a model [31]. An important body of work by the Goodhill group developing statistical models of cues binding to receptors on the growth cone [32], and used these models to determine the constraints on sensing from the shape of the gradient [33]. Further, it was found that spatial sensing appeared to be more efficient than temporal sensing for experimental cue concentrations [34]. Katz and Lasek [35] have also identified some required constraints to produce ordered axonal arrangements from growth modeled as a simple random walk.

Since the biochemistry of the growth process is extremely complex, so far it has only been possible to model the actual biophysical mechanisms in some special cases. For example, work by Segev and Ben-Jacob [36] modeled self-wiring of a neural network with growth cones moving in the presence of diffusive factors. They proposed the use of graph-theoretic tools e.g. counting neighbors to characterize the networks formed as a possible means of experimental comparison. Simulations of the dynamics of multiple axons in complex domains with multiple guidance factors has been developed by van Ooyen's group [37]. Sakumura and collaborators [38] and Jilkin and collaborators [39] have formulated models that attempt to predict the response of a growth cone to a chemical gradient. Mogilner and Rubenstein [40] have constructed a detailed mechanical model of filopodia to determine the optimal length. In recent work Padmanabhan and Goodhill incorporated a molecular feedback loop mechanism on pathways that are important for cytoskeletal control in the growth cone [41]. This model creates unimodal or bistable states of growth for growth cones depending on the rates of point contact assembly. Coupled with a random walk model that gives angular distributions, the model could be used in a random walk with rest periods, where the bouts of growth and rest are based on changing results of this bistable switch model as the growth cone interacts with its environment [41].

A different approach, uses Langevin type and/or Fokker-Planck equations to simulate axonal growth using stochastic forces. By explicitly deriving probability distributions of the axonal growth process as the solution of a Fokker-Planck equation, it becomes possible to falsify causal mechanisms from experimentally observed results. For example, Hentschel and van Ooyen [42] showed that a combination of chemoattractant and chemorepellent factors could explain the bundling, guidance and then de-bundling of axons towards a target region. A more sophisticated model, incorporating extension and retraction of filipodia and binding of ligands to the growth cone, was utilized by Goodhill and collaborators [43] to simulate axonal trajectories in the presence

of a chemical gradient. Maskery and Shinbrot [44] established that Langevin simulations predict a minimum detectable gradient. Pearson and collaborators [45] solved the Fokker-Planck equation to predict the geometric features of axonal trajectories in the absence of external cues. Betz and collaborators [46] used Fokker-Planck to quantify the bimodal growth behavior of the leading edge lamellipodia emerging from the internal bistable polymerization processes in the growth cone.

In our previous work we showed that the Fokker-Planck equation provides a general framework for predicting the growth cone dynamics and for describing the role that different types of environmental cues have on axonal growth. For example, in our earlier work we have shown that axonal dynamics for cortical neurons grown on glass substrates coated with poly-D-lysine (PDL) is governed by a V-shaped potential, which results in a regulatory mechanism for the axonal growth rates on these surfaces [47]. We have used also the Langevin and Fokker-Planck equations to quantify axonal growth on surfaces with ratchet-like topography (asymmetric tilted nanorod: nano-ppx surfaces) [48, 49]. We have shown that the axonal growth is aligned with a preferred spatial direction as a result of a “deterministic torque” that drives the axons to directions determined by the substrate geometry. We have also measured the angular distributions and the coefficients of diffusion and angular drift on these substrates [49].

3. Neuronal growth on surfaces with periodic geometrical patterns

In a series of recent papers we have shown that periodic geometrical patterns impart strong directional bias to axonal growth [50-55]. To prepare the periodic geometrical patterns we use a simple fabrication method based on imprinting diffraction grids with different grating constants onto poly-D-lysine (PDL) coated polydimethylsiloxane (PDMS) substrates (details given in [53-55]). The PDMS growth substrates thus consist of periodic parallel ridges separated by throughs Fig. 1a.

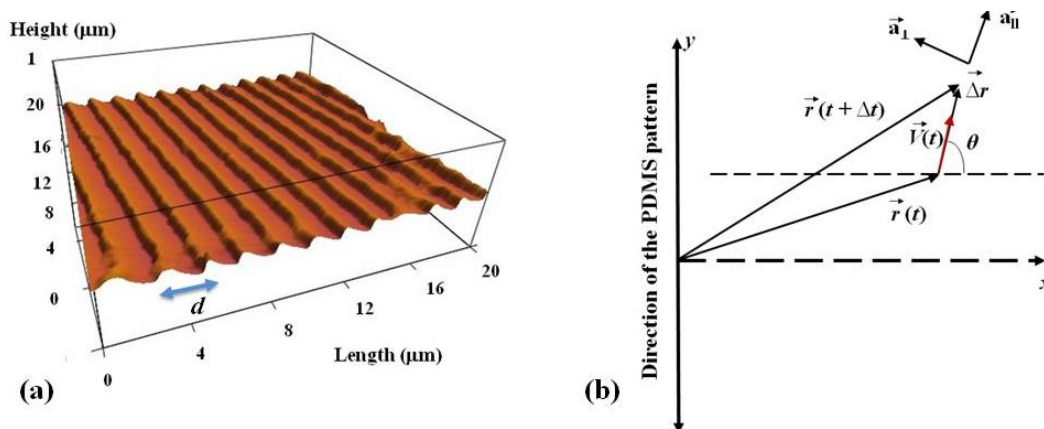


Figure 1. (a) Atomic Force Microscope (AFM) topographic image of a PDL coated PDMS patterned surface. The image shows that the micropatterns are periodic in the x direction with the spatial period $d = 2 \mu\text{m}$ and have a constant depth of approximately $0.5 \mu\text{m}$. (b) Coordinate system and the definition of the angular coordinate θ . The x axis is defined as the axis perpendicular to the direction of the PDMS patterns. The directions for the parallel and perpendicular components of the acceleration are also defined in the figure.

Each surface is characterized by the pattern spatial period d defined as the distance between two neighboring ridges (Fig. 1a). We create a series of different types of surfaces with pattern

spatial distances in the range $d = 1 \mu\text{m}$ to $10 \mu\text{m}$ (in increments of $1 \mu\text{m}$). The parameter d is measured by atomic force microscope (AFM) for each surface. The cells used in these studies are cortical neurons obtained from embryonic day 18 rats. For cell dissociation, culture and imaging we have used established protocols presented in our previous work [56-60]. Fluorescence images have been measured by staining the neurons with Fluorescence Tracker Green [56-58]. We measure angular distribution of neuronal growth on micropatterned PDMS surfaces using the coordinates defined in Fig. 1b.

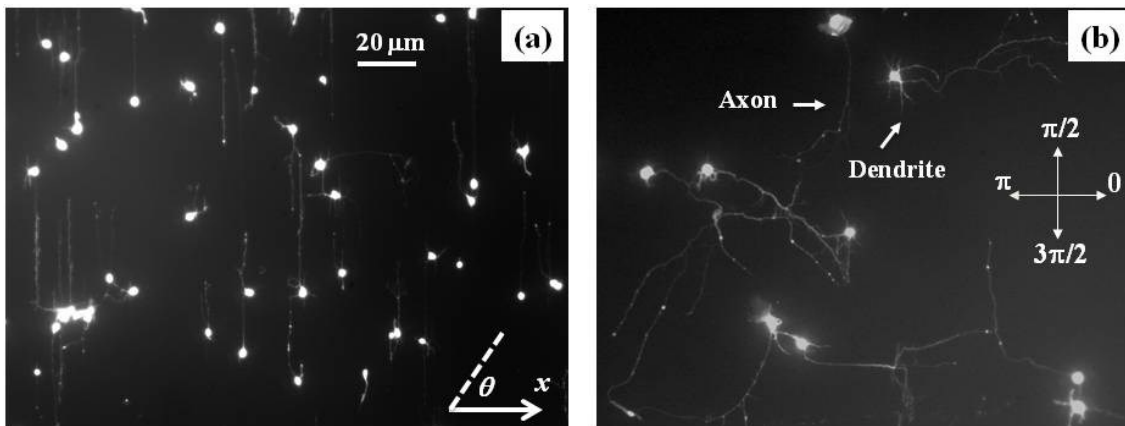


Figure 2. Fluorescence images showing examples of axonal growth for cortical neurons cultured on a PDL coated PDMS surfaces with periodic micropatterns. (a) Example of neuronal growth and axonal alignment for cortical neurons grown on PDMS substrates with pattern spatial period: $d = 4 \mu\text{m}$. (b) Example of axonal growth for cortical neurons cultured on flat (un-patterned) PDMS substrate coated with PDL (control substrate). Cortical neurons typically grow a long process (the axon) and several minor processes (dendrites). These processes are shown in (b). The axons is identified by its morphology and the growth cone is identified as the tip of the axon. The angular coordinate θ used in this paper is defined in (a). The directions corresponding to $\theta = 0, \pi/2, \pi,$ and $3\pi/2$ are also shown in (b). All angles are measured with respect to the x axis, defined as the axis perpendicular to the direction of the PDMS patterns (see Fig. 1b). Both images are captured 32 hrs after neuron plating. For micropatterned surfaces the axons tend to align along the direction the micropatterns as shown on (a). In contrast, axons growing on un-patterned PDMS display no directional alignment as shown in (b). The scale bar shown in (a) is the same for all images.

Fig. 2a shows an example of axonal growth for neurons, cultured on a PDL coated PDMS surfaces with pattern spatial period: $d = 4 \mu\text{m}$. Fig. 2b shows neuronal growth on a control PDL coated PDMS surface with no surface patterning. We have previously demonstrated that axons tend to grow parallel to the periodic micro-patterns (Fig. 2a), and that the axonal alignment depends on the pattern spatial distance d : axons display maximum alignment for surfaces where d matches the linear dimension of the growth cone l , where l is in the range 2 to $6 \mu\text{m}$ [50]. In previous work [51, 52] we have also demonstrated that the axons tend to grow on top of the semi-cylindrical micropatterns.

4. Langevin and Fokker-Planck formalism for modelling axonal dynamics

Axonal growth arises as the result of an interplay between deterministic and stochastic components of growth cone motility [42-55]. Deterministic influences include, for example the presence of preferred directions of growth along specific geometric patterns on substrates, while stochastic components come from the effects of polymerization of cytoskeletal elements (actin filaments and microtubules), neuron signaling, low concentration biomolecule detection, biochemical reactions within the neuron, and the formation of lamellipodia and filopodia [1-3, 6-9, 61-64]. The resultant growth cannot be predicted for individual neurons due to this stochastic-deterministic interplay, however the growth dynamics for a population of neurons can be modeled by probability functions that satisfy a set of well-defined stochastic differential equations. In particular, Langevin and Fokker-Planck equations [65] provide a powerful framework for modeling the interplay between the deterministic and stochastic components of axonal dynamics.

Langevin equation for axonal growth on glass

In previous work [50] we have shown that axonal dynamics on uniform glass surfaces is described by an Ornstein-Uhlenbeck (Brownian) process, defined by a *linear* Langevin equation for the velocity \vec{V} :

$$\frac{d\vec{V}}{dt} = -\gamma_g \cdot \vec{V} + \vec{\Gamma}(t) \quad (1)$$

The first term in Eq. (1) represents the deterministic term, and γ_g is a constant damping coefficient. The second term $\vec{\Gamma}(t)$ represents the stochastic change in velocity, which is described by Gaussian white noise. From Eq. (1) we can calculate the mean square length and the velocity autocorrelation function [50]. By comparing the theoretical predictions with the experimentally measured distributions for these parameters we can extract the two fundamental parameters that characterize the Brownian motion of axons on glass surfaces: the diffusion coefficient D and the characteristic time for the exponential decay of the velocity autocorrelation function: $\tau_g = 1/\gamma_g$. For cortical neurons grown on PDL coated glass these parameters are [50]: $D = (16 \pm 2) \mu\text{m}^2/\text{hr}$ and $\gamma_g = (0.1 \pm 0.05) \text{hr}^{-1}$.

Langevin equations for axonal growth on patterned PDMS surfaces

Axonal dynamics on micropatterned PDMS surfaces is described by a non-linear Langevin equation:

$$\vec{a}(\vec{V}, t) \equiv \frac{d\vec{V}}{dt} = \vec{a}_d(\vec{V}, t) + \vec{\Gamma}(\vec{V}, t) \quad (2)$$

where $\vec{a}_d(\vec{V}, t)$ is the deterministic component of the axonal motion and the term $\vec{\Gamma}(\vec{V}, t)$ represents the stochastic contributions. The acceleration of axons is decomposed into a component parallel to the direction of motion $a_{d,\parallel}(\vec{V}, t)$, and a component perpendicular to this direction $a_{d,\perp}(\vec{V}, t)$ (Fig. 1b). A separate analysis of the two motions leads to the following non-linear Langevin equations for the two components of the acceleration [50]:

$$a_{\parallel}(V, \theta, t) \equiv \left(\frac{d\vec{V}}{dt} \right)_{\parallel} = a_0 \cdot |\sin \theta| - \gamma_1 \cdot V - \gamma_2 \cdot V^2 + \Gamma_{\parallel}(t) \quad (3)$$

$$a_{\perp}(V, \theta, t) \equiv \left(\frac{d\vec{V}}{dt} \right)_{\perp} = a_1 \cdot \cos \theta + \Gamma_{\perp}(t) \quad (4)$$

In the above expressions θ represents the growth angle defined in Fig. 1b and Fig. 2, V is the growth cone speed, and a_0, a_1, γ_1 , and γ_2 are velocity-independent parameters that characterize axonal dynamics on substrates with periodic geometries. Γ_{\parallel} and Γ_{\perp} are the stochastic contributions for parallel and perpendicular growth. We have shown that all these parameters are experimentally measurable [50].

Equations (3)-(4) show that the axonal dynamics on surfaces with periodic geometries is described by non-linear Langevin equations, involving quadratic velocity terms and non-zero coefficients for the angular orientation of the growing axon. There are some very important consequences for axonal growth that follow from this type of dynamics. In particular, Eqns. (3)-(4) show angular alignment of axonal growth on micropatterned PDMS surfaces. The magnitude of the perpendicular acceleration $a_{d,\perp}(\theta)$ has a maximum value when the direction of axonal growth is perpendicular to the surface pattern (i.e. for $\theta = 0$ and $\theta = \pi$ in Fig. 2), and it equals zero when the axon grows along the pattern ($\theta = \pi/2$ and $\theta = 3\pi/2$). This shows that the perpendicular component of acceleration $a_{d,\perp}(\vec{V}, t)$ tends to *align the growth cone along the direction* of the pattern. The net effect is that of a deterministic torque (quantified by the parameter a_1) which rotates the growth cone towards the surface geometrical pattern. Fig. 3 shows examples of angular (Fig. 3a) and speed (Fig. 3b) distributions for axonal growth on a surface with $d = 4 \mu\text{m}$.

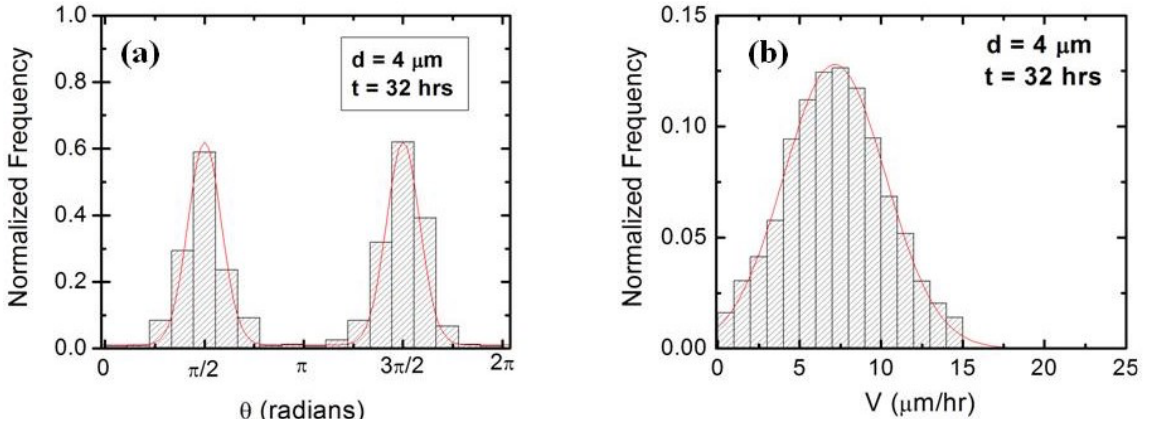


Figure 3. (a) Example of normalized experimental angular distributions for axonal growth for neurons cultured on micropatterned PDMS surfaces with pattern spatial period $d = 4 \mu\text{m}$. The vertical axis (labeled Normalized Frequency) represents the ratio between the number of axonal segments growing in a given direction and the total number N of axon segments. Each axonal segment is of $20 \mu\text{m}$ in length [50-53]. For (a) we have analyzed $N = 510$ different axon segments (total of 67 axons). The data shows that the axons display strong directional alignment along the surface patterns (peaks at $\theta = \pi/2$ and $\theta = 3\pi/2$). (b) Example of normalized speed distributions for growth cones measured on a micropatterned PDMS surfaces with pattern spatial period $d = 4 \mu\text{m}$. All distributions show data collected at $t = 32$ hrs after neuron plating. The

continuous red curves in each figure represent fit to the data with the Fokker-Planck model discussed in the text (see Eqns. 9 and 11).

Another prediction of the model described by Eqns. (3) and (4) is that the growth cone reaches a terminal speed along the direction pattern, which can be found the condition that the average acceleration in Eq. (3) equals zero. This gives the following analytic expression for the terminal speed of the growth cone [50]:

$$V_{ter} = \sqrt{\frac{a_0}{\gamma_2} \cdot |\sin \theta| + \frac{\gamma_1^2}{4\gamma_2^2}} - \frac{\gamma_1}{2\gamma_2} \quad (5)$$

Eqn. (5) has a number of features that can be tested experimentally. First, the growth cones reaches terminal speed only for growth angles $\theta \neq 0$. In addition, the terminal speed depends only on the ratios of the growth parameters a_0/γ_2 , and γ_1/γ_2 which ultimately depend on the pattern spatial period d . We have experimentally verified these predictions in reference [50]. In particular, we have measured the values for the terminal speed on surfaces with different d and have shown good agreement with the values predicted by Eqn. (5).

An important consequence of the non-linear Langevin equations (3) and (4) is that axonal growth displays a cross-over from Brownian motion at earlier to a super-diffusion regime at later times. The super-diffusive dynamics is characterized by non-Gaussian speed distributions (Fig. 4a) and power law increase of the axonal mean square length with time (Fig. 4b).

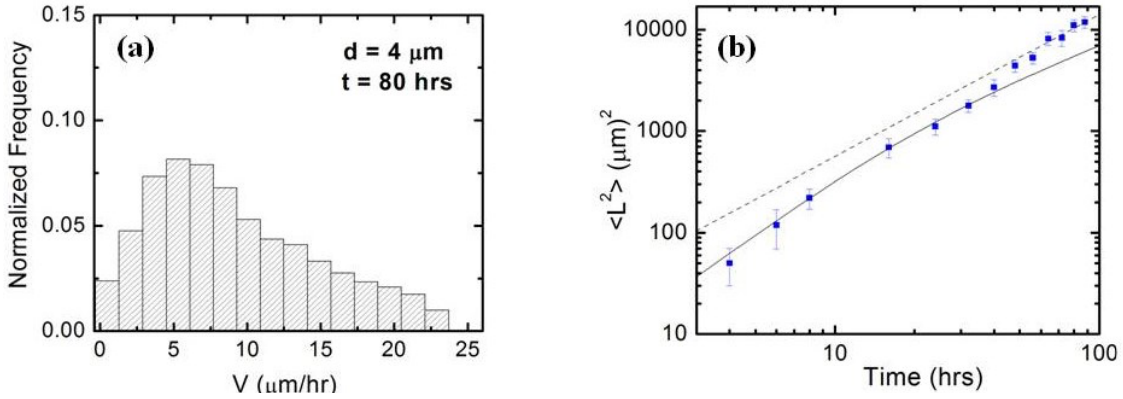


Figure 4. (a) Example of non-Gaussian speed distribution measured for axons grown on a surface with pattern spatial period $d = 4 \mu\text{m}$, at $t = 80$ hrs after neuron plating ($N = 582$ different axon segments (total of 73 axons)). (b) (adapted from ref. [51]). Log-Log plot showing the variation of the axonal mean square length with time. The continuous curve represents the fit to the data measured at $t < 48$ hrs with the prediction of the theoretical model describing Brownian motion [51]. The dotted curve represents the fit to the data points measured for $t \geq 48$ hrs with a power-law function with coefficient ~ 1.4 , which is characteristic to a super-diffusive process [51].

The observed transition between the diffusive and super-diffusive behavior in the case of axonal motion suggests the existence of long-range spatial and temporal correlations in the underlying dynamics [51]. However, the details of how this process emerges from cell-cell and

cell-substrate interactions are currently not well understood and are subject to future investigations (see section on future work below).

Fokker-Planck equations

In a series of recent papers [50-55] we have shown that the axonal dynamics on surfaces with periodic geometries is completely described by the following system of Fokker-Planck equations:

Spatial probability distributions:

$$\frac{\partial}{\partial t} p(\vec{r}, t) = D \cdot \nabla^2 p(\vec{r}, t) + \frac{1}{\gamma} \nabla \cdot (p(\vec{r}, t) \cdot \nabla V(\vec{r})) \quad (6)$$

1-dimensional (1D) stationary solutions for motion along micropatterns:

$$p(\vec{r}, t) = A \cdot p(x, t), \quad \text{with } p(x) = (1/Z) \cdot \exp(-(V \cdot x^2 + V_{\text{ext}}(x))/D \cdot \gamma) \quad (7)$$

In Eqns. (7) and (8) $p(\vec{r}, t)$ is the spatial probability distribution, D the represents the diffusion (cell motility) coefficient, γ is the damping coefficient (friction constant of the corresponding Langevin equation), and $V(\vec{r})$ is the effective potential that determines the axonal dynamics. In the case of growth on periodic micropatterns the probability distribution is determined by $p(x, t)$ which represents the 1D solution of Eqn. (6) along the axonal growth direction (A and Z are overall normalization constant). The growth potential can be written as: $V(\vec{r}) = V_{\text{ext}}(\vec{r}) + V_F(\vec{r}) + V_{\text{int}}(\vec{r}, p)$, where $V_{\text{ext}}(\vec{r})$ is the neuron-substrate coupling potential (external potential imposed by the substrate geometry), $V_F(\vec{r})$ is the potential responsible for the closed-loop feedback (to be discussed below), and $V_{\text{int}}(\vec{r}, p)$ is the neuron-neuron interaction potential (quantifies the interactions between neuronal cells). The form of these three potentials has been studied in [55].

Speed probability distributions:

$$\frac{\partial}{\partial V} p(V, t) = \frac{\partial}{\partial V} [\gamma_s \cdot (V - V_s) \cdot p(V, t)] + \frac{\sigma^2}{2} \cdot \frac{\partial^2}{\partial V^2} p(V, t) \quad (8)$$

Stationary solutions:

$$p(V) = B \cdot \exp\left(-\frac{\gamma_s}{\sigma^2} \cdot (V - V_s)^2\right) \quad (9)$$

In Eqn. (8) and (9) $p(V, t)$ is the speed distribution of axonal growth, γ_s is the constant damping coefficient of the corresponding Langevin equation for speed ($\gamma_s = 1/\tau$ where τ is the characteristic decay time), V_s is the average stationary speed of the axons and σ is the strength for an uncorrelated Wiener process with Gaussian white noise. B is an overall normalization constant obtained from the condition: $\int_0^\infty p(V) \cdot dV = 1$

Angular probability distributions:

$$\frac{\partial}{\partial t} p(\theta, t) = \frac{\partial}{\partial \theta} [-\gamma_{\theta} \cdot \cos \theta(t) \cdot p(\theta, t)] + D_{\theta} \cdot \frac{\partial^2}{\partial \theta^2} p(\theta, t) \quad (10)$$

Stationary solutions:

$$p(\theta) = C \cdot \exp\left(\frac{\gamma_{\theta}}{D_{\theta}} \cdot |\sin(\theta)|\right) \quad (11)$$

In Eqn. (10) and (11) $p(\theta, t)$ is the probability distribution for the growth angle θ , D_{θ} represents the effective angular diffusion (cell motility) coefficient, and $\gamma_{\theta} \cdot \cos \theta(t)$ corresponds to a “deterministic torque” representing the tendency of the growth cone to align with the preferred growth direction imposed by the surface geometry. C is a normalization constant obtained from the normalization condition: $\int_0^{2\pi} p(\theta) \cdot d\theta = 1$.

The absolute value $|\sin \theta|$ in Eq. 11 reflects the symmetry of the growth around the x axis: the angular distributions centered at $\theta = \pi/2$ and $\theta = 3\pi/2$ are symmetric with respect to the directions $\theta = \pi$ and $\theta = 0$ (Figs. 1 and 2). This is a consequence of the fact that there is no preferred direction along the PDMS pattern (Fig. 1), and this feature applies to all types of micropatterned PDMS surfaces. We also note that the deterministic torque has a maximum value if the growth cone moves perpendicular to the surface patterns ($\theta = 0$ or $\theta = \pi$), in which case the cell-surface interaction tend to align the axon with the surface pattern. The torque is zero for an axon moving along the micropattern.

We have shown that the model given by Eqns. (6) to (11) fully accounts for the all experimental data of neuronal growth on micropatterned PDMS surfaces. In particular, we have used this model to extract key dynamical parameters of axonal motion: diffusion (cell motility) coefficients, speed and angular distributions, mean square displacements, and deterministic torque. For example, Fig. 3 shows normalized angular and speed distributions measured experimentally as well as fit to the data using Eqns. (9) and (11) (continuous red curves). Typical values obtained for the growth parameters are: diffusion coefficient $D = (22 \pm 4) \mu\text{m}^2/\text{hr}$, coefficient for the “deterministic” alignment torque $\gamma_{\theta} = (0.13 \pm 0.04) \text{hr}^{-1}$, and characteristic time for axonal alignment: $\tau = (5.1 \pm 0.8) \text{hr}^{-1}$. We have performed a detailed analysis of how these parameters depend on the type of substrate, growth time, and chemical modification of the neurons [51-55]. These results show that the dynamics of the ensemble of axons can be described phenomenologically if each growth cone is modeled as an automatic controller with a closed feedback loop [55]. Growth alignment is fully determined by the surface geometry, and the pattern spatial period d plays the role of a control parameter. In particular, we have performed experiments which demonstrate that the disruption of cytoskeletal dynamics through neuronal treatment with different chemical compounds alters the feedback loop of the cellular controller [52-55].

5. Mechanical model of axonal growth on periodic patterns

The phenomenological models discussed in the previous sections form a basis for quantifying cell-cell and cell-surface interactions, and ultimately for describe how the formation of neuronal network emerges from collective biophysical processes of single cells. In particular, the Fokker-Planck dynamics can be justified by a simple mechanical model that takes into account the cell-substrate interactions [54, 55]. The model considers the bending-induced strained

sustained by the axon while growing on the semi-cylindrical pattern of radius R : axonal adhesion to the surface leads to axonal bending, which in turn leads to increased mechanical strain energy in the axon cytoskeleton. The mechanical strain energy E depends on the axon bending modulus F , and the local surface curvature $K(\theta, R)$ [54, 55] :

$$E = \frac{1}{2} F \cdot K^2(\theta, R) \quad (12)$$

In the case of axonal growth on the micropatterned surfaces, the curvature of an axon wrapped at angle α around the cylindrical pattern is given by:

$$K^2(\theta, R) = \frac{|\cos(\alpha)|}{R^2} \equiv \frac{|\sin(\theta)|}{R^2} \quad (13)$$

For the stationary growth described by Eqn. (9) and (11) one can assume a Boltzmann distribution for the probability of axon growing in a given direction [55]:

$$p(\theta) = A_1 \cdot \exp\left(-\frac{E}{E_0}\right) \quad (14)$$

where E_0 is the characteristic energy scale for axonal bending, and A_1 is an overall normalization constant. From Eqns. (12)-(14) and using our convention for the angular variable θ (**Fig. 1 b**), we get:

$$p(\theta) = A_2 \cdot \exp\left(\frac{F}{E_0 \cdot R^2} \cdot |\sin(\theta)|\right) \quad (15)$$

By comparing the solution of this simple mechanical beam model (Eq. 15) with the solutions of the Fokker-Planck Eqns. (7) and (11), and using the experimental measured values for the radius R of curvature of the micropattern and the growth parameters D_θ and γ_θ one can extract the bending modulus of the axon. Typical values for the bending modulus are: $F \approx 23 \text{ J} \cdot \mu\text{m}^2$ for untreated neurons, and $F \approx 17 \text{ J} \cdot \mu\text{m}^2$ for neurons in which the cytoskeletal dynamics was inhibited by chemical modification [54, 55].

These results show that axonal stiffness and substrate curvature can act together to direct axonal growth. This work could be extended to account for the explicit dependence of the growth parameters on the biomechanical and geometrical guidance cues, such as changes in the geometry or stiffness of the growth substrate, or external forces. For example, a model for the cooperative motion for ensembles of closed packed cells was proposed by C. Marchetti and collaborators [66]. This model incorporates contractile forces and effective cellular polarization as internal variables, which generate waves of collective cellular motion. Continuum mechanical models that account for the interplay between cell-substrate couplings and the cell biomechanical properties have also been proposed [67- 71]. The parameters for these models can be measured experimentally by a combination of Atomic Force Microscopy (AFM) and Traction Force Microscopy (TFM) measurements as described below.

6. Combined Traction Force - Atomic Force microscopy measurements

Although it is generally accepted that mechanics plays an important role in cellular dynamics and function, this field is still underdeveloped compared to other areas of biophysics, and we are only beginning to understand how biomechanical processes affect the development and behavior of cells [17, 72 - 79]. In

particular, despite recent impressive advances in our understanding of how neurons grow and form functional connections, a fully quantitative description of axonal dynamics, which takes into account the interactions between the cell and the growth environment is still missing. We have shown that Fokker-Planck equations provide a robust framework for quantifying the deterministic and stochastic components of axonal motion. These equations enable accurate prediction of growth cone dynamics and provide a systematic approach for analyzing the respective roles played by external biochemical, mechanical, and geometrical cues. In the case of neuronal growth on surfaces with periodic geometrical patterns, axonal alignment is a consequence of a simple mechanical model that considers the bending of the axon imparted by the surface geometry: axonal adhesion to growth surface leads to axonal bending, which in turn leads to increased mechanical strain energy in the axon cytoskeleton. Future work will use these phenomenological models as a basis for quantifying cell-cell and cell-surface interactions, and ultimately for describing how the formation of neuronal network emerges from collective biophysical processes of single cells.

One very promising direction of research is to develop a comprehensive model of neuronal growth as a function of experimentally relevant surface properties (geometry, substrate stiffness), cell-substrate traction forces, adhesion strengths, and cellular biomechanical properties (elastic modulus and dynamics of the cytoskeletal elements). To this end we have recently started to perform combined Atomic Force (AFM) – Traction Force Microscopy (TFM) experiments to elucidate the relationships between neuronal biomechanical properties and the mechanical and geometrical features of the growth substrate [80]. The goals are to measure biomechanical properties of individual neurons, the cell-substrate interactions and to identify the quantitative relationships between cellular mechanics and the internal mechanisms that determine neuronal structure and function.

The particular capabilities of the AFM, such as nanometer-scale spatial resolution and positioning on the cell surface, high degree of control over the magnitude (sub- nN resolution) and orientation of the applied forces, minimal sample damage, and the ability to image and interact with cells in physiologically relevant conditions make this technique particularly suitable for measuring biomechanical properties of neurons. In previous work [56-60] we have combined fluorescence microscopy with AFM force mapping to produce systematic, high-resolution elasticity and fluorescence maps for several types of neuronal cells, including cortical, embryonic cDRGs, and P-19 (mouse embryonic carcinoma stem cells). We have also performed combined AFM and fluorescence experiments to investigate the relationship between external temperature, soma volume and elastic modulus for cortical neurons [58, 59]. Our results show an increase by a factor of 2 in the soma elastic modulus as the ambient temperature decreases from physiological (37°C) to room (25°C) temperature [59]. We have also found that the soma volume is increasing with temperature by a factor of 1.3 during the temperature sweep from 25°C to 37°C [59]. Our results show that both the variations in elastic modulus and cell volume are highly reduced if the activity of molecular motors inside the neurons is inhibited, through treatment with chemical compounds (Taxol and Blebbistatin) that are known to have an inhibitory effect on the cytoskeleton dynamics [58, 59].

Traction Force Microscopy (TFM) is the method of choice for measuring traction stresses and forces generated by motile cells, and for tracking cell–substrate interactions [8-10, 13, 15, 17]. In TFM a mechanically compliant substrate is deformed by cells and the deformations are measured using fluorescent beads embedded in the substrate. TFM experiments performed on neurons have demonstrated that growth cones exert traction forces during axonal extension that result in increased tension along the axons [10, 13, 15]. It has been suggested that mechanical

tension is an important factor that regulate axonal dynamics and the formation of the neuronal networks [8-16].

Fig. 5 shows examples of AFM and TFM images obtained on the inverted stage of our Asylum Research AFM.

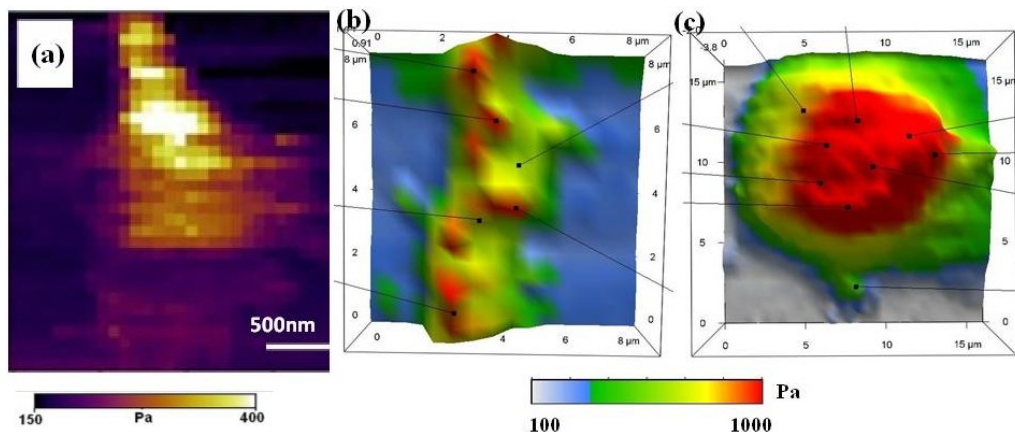


Figure 5. (a) Two-dimensional AFM force map of an axonal growth cone. The growth cone stiffness at each indentation point is shown by the color scale. (b), (c): Combined AFM-TFM image of the axon (b) and soma (c) for a neuronal cell. The arrows in each figure show the points of maximum coupling between the cell and the growth substrate. The stiffness scale bar is the same for both (b) and (c).

Using combined TFM-AFM measurements we can relate changes in neuron volume, elastic modulus, and cell deformations to forces/stresses exerted by the cell on the surface [80]. In principle, these experiments will enable us to measure how changes in cell-substrate coupling forces and neuron biomechanical properties affect cytoskeletal dynamics and axonal motion, and thus to better understand the interplay among the many factors that govern neuronal growth and the formation of neuronal networks.

7. Conclusions and Future work

In future work, combined AFM, TFM and fluorescence measurements will allow us to measure the density and location of curvature sensing proteins and integrins in experiments where the growth cone filopodia and lamellipodia wrap around the ridges of micropatterns. Neuron biomechanical properties (elastic modulus, cytoskeletal dynamics, changes in volume and cell-substrate contact area) are determined by simultaneous AFM measurements. By combining the experimental approach with continuum mechanics models, we aim to develop a detailed inhomogeneous mechanical model of neuronal growth that incorporates linear elasticity, cytoskeletal dynamics, and cell-substrate interactions. We emphasize that *all the input parameters* in the model will be experimentally measured. The predictions of the model could also be tested experimentally by varying the external stimuli and at each iteration the model could be refined to account for the observations, and to predict a larger class of biomechanical and biophysical phenomena. The end goal of this effort is to connect the Fokker-Planck formalism to computationally predictable and experimentally measurable morphological changes of the cell as well as with external forces.

These results presented above support the hypothesis that neurons follow mechanical and geometrical patterns through a contact – guidance mechanism [8, 9, 20, 81-83]. Contact guidance is the behavior displayed by many different types of cells which can change their motion in response to geometrical cues present in the surrounding environment. This property has been observed for several types of cells including neurons, fibroblasts, and tumor cells [20, 81-83]. Growth cones develop several different types of curvature sensing proteins and integrins that act as sensors of geometrical and mechanical cues and are involved in the generation of traction forces. Moreover, the degree of directional alignment of cellular motion is increasing with the increase in the density of curvature sensing proteins [81-83]. Consequently, contact guidance predicts that high-curvature geometrical features such as ridges on growth substrates will impart higher forces to the focal contacts of filopodia wrapped over these features, compared to the low-curvature patterns. These predictions could be investigated in combined AFM - TFM experiments as described above.

In conclusion these novel theoretical and experimental methods will allow us to investigate the collaborative mechanisms among many of the basic biophysical factors that govern the neuronal development and function. Furthermore, these models could also be applied to other types of cells to give new insight into the nature of cellular motility. In principle these future investigations will enable researchers to quantify the influence of environmental cues (geometrical, mechanical, biochemical) on cellular dynamics, and to relate the observed cell motility behavior to cellular processes, such as cytoskeletal dynamics, cell-surface interactions, and signal transduction mechanisms.

Acknowledgement. The author thanks Dr. Elise Spedden for her involvement in the initial stages of the combined AFM-TFM project. The author gratefully acknowledges financial support for this work from National Science Foundation (DMR 2104294), Tufts Springboard and Tufts Summer Faculty Fellowship Award.

References

1. Lowery, L.A. and D. van Vactor, *The trip of the tip: understanding the growth cone machinery*. Nature Rev. Mol. Cell Biology, 2009. **10**: p. 332-343.
2. Huber, A.B., A.L. Kolodkin, D.D. Ginty, and J.F. Cloutier, *Signaling at the growth cone: ligand-receptor complexes and the control of axon growth and guidance*. Annu Rev Neurosci, 2003. **26**: p. 509-63.
3. Rosoff, W.J., J.S. Urbach, M.A. Esrick, R.G. McAllister, L.J. Richards, and G.J. Goodhill, *A new chemotaxis assay shows the extreme sensitivity of axons to molecular gradients*. Nature Neuroscience, 2004. **7**(6): p. 678-682.
4. Staii, C., C. Viesselmann, J. Ballweg, L. Shi, G.-Y. Liu, J.C. Williams, E.W. Dent, S.N. Coppersmith, and M.A. Eriksson, *Distance Dependence of Neuronal Growth on Nanopatterned Gold Surfaces*. Langmuir, 2011. **27**: p. 233-239.
5. Staii, C., C. Viesselmann, J. Ballweg, L.F. Shi, G.Y. Liu, J.C. Williams, E.W. Dent, S.N. Coppersmith, and M.A. Eriksson, *Positioning and Guidance of Neurons on Gold Surfaces by Directed Assembly of Proteins using Atomic Force Microscopy*, Biomaterials, 2009. **30**: p. 3397-3404.

6. Dickson, B.J., *Molecular mechanisms of axon guidance*. Science, 2002. **298**(5600): p. 1959-1964.
7. Dickson, B.J. and K.A. Senti, *Axon guidance: Growth cones make an unexpected turn*. Current Biology, 2002. **12**(6): p. R218-R220.
8. Franze, K., *The mechanical control of nervous system development*. Development, 2013. **140** (15): p. 3069-77.
9. Franze, K. and J. Guck, *The biophysics of neuronal growth*. Reports on Progress in Physics, 2010. **73**(9): p. 094601.
10. Koch, D., W.J. Rosoff, J. Jiang, H.M. Geller, and J.S. Urbach, *Strength in the periphery: growth cone biomechanics and substrate rigidity response in peripheral and central nervous system neurons*. Biophys J, 2012. **102**(3): p. 452-60.
11. Lu, Y.B., K. Franze, G. Seifert, C. Steinhauser, F. Kirchhoff, H. Wolburg, J. Guck, P. Janmey, E.Q. Wei, J. Kas, and A. Reichenbach, *Viscoelastic properties of individual glial cells and neurons in the CNS*. Proc Natl Acad Sci U S A, 2006. **103**(47): p. 17759-64.
12. P.C. Georges, W.J. Miller, D.F. Meaney, E.S. Sawyer, and P.A. Janmey, *Matrices with compliance comparable to that of brain tissue select neuronal over glial growth in mixed cortical cultures*. Biophys J, **90**(8), p. 3012-8, (2006).
13. Hyland, C., A.F. Mertz, P. Forscher, and E. Dufrene, *Dynamic peripheral traction forces balance stable neurite tension in regenerating Aplysia bag cell neurons*. Nature Sci Rep, 2014. **4**: p. 4961.
14. Lamoureaux, P., G. Ruthel, R.E. Buxbaum, and S.R. Heidemann, *Mechanical tension can specify axonal fate in hippocampal neurons*. Journal Cell Biology 2002. **159**: p. 499-508.
15. Polackwich, R.J., D. Koch, R. McAllister, H.M. Geller, and J.S. Urbach, *Traction force and tension fluctuations in growing axons*. Front Cell Neurosci, 2015. **9**: p. 417.
16. Wen, Z. and J.Q. Zheng, *Directional guidance of nerve growth cones*. Curr Opin Neurobiol, 2006. **16**(1): p. 52-8.
17. Roca-Cusachs, P., V. Conte, and X. Trepac, *Quantifying forces in cell biology*. Nat Cell Biol, 2017. **19**(7): p. 742-751.
18. Francisco, H., B.B. Yellen, D.S. Halverson, G. Friedman, and G. Gallo, *Regulation of axon guidance and extension by three-dimensional constraints*. Biomaterials, 2007. **28**(23): p. 3398-407.
19. Farrukh, A., S. Zhao, and A. del Campo, *Microenvironments Designed to Support Growth and Function of Neuronal Cells*. Frontiers in Materials, 2018. **5**(62): p. 1-22.
20. S.W. Moore and M.P. Sheetz, *Biophysics of substrate interaction: influence on neural motility, differentiation, and repair*. Dev Neurobiol, **71**(11), p. 1090-101, (2011).
21. Y.W. Fan, F.Z. Cui, S.P. Hou, Q.Y. Xu, L.N. Chen, and I.S. Lee, *Culture of neural cells on silicon wafers with nano-scale surface topograph*. J Neurosci Methods, **120**(1), p. 17-23, (2002).
22. D.Y. Fozdar, J.Y. Lee, C.E. Schmidt, and S. Chen, *Selective axonal growth of embryonic hippocampal neurons according to topographic features of various sizes and shapes*. Int J Nanomedicine, **6**, p. 45-57, (2011).
23. F. Johansson, P. Carlberg, N. Danielsen, L. Montelius, and M. Kanje, *Axonal outgrowth on nano-imprinted patterns*. Biomaterials, **27**(8), p. 1251-8, (2006).
24. A. Rajnicek and C. McCaig, *Guidance of CNS growth cones by substratum grooves and ridges: effects of inhibitors of the cytoskeleton, calcium channels and signal transduction pathways*. J Cell Sci, **110** (Pt 23), p. 2915-24, (1997).

25. S.R. Hart, Y. Huang, T. Fothergill, D.C. Lumbard, E.W. Dent, and J.C. Williams, *Adhesive micro-line periodicity determines guidance of axonal outgrowth*. Lab Chip, **13**(4), p. 562-9, (2013).
26. M. Song and K.E. Uhrich, *Optimal micropattern dimensions enhance neurite outgrowth rates, lengths, and orientations*. Ann Biomed Eng, **35**(10), p. 1812-20, (2007).
27. L. Kam, W. Shain, J.N. Turner, and R. Bizios, *Axonal outgrowth of hippocampal neurons on micro-scale networks of polylysine-conjugated laminin*. Biomaterials, **22**(10), p. 1049-54, (2001).
28. M.J. Katz, E.B. George, and L.J. Gilbert, *Axonal elongation as a stochastic walk*. Cell Motil, **4**, p. 351-370, (1984).
29. D.J. Odde, E.M. Tanaka, S.S. Hawkins, and H.M. Buettnner, *Stochastic dynamics of the nerve growth cone and its microtubules during neurite outgrowth*. Biotechnol Bioeng, **50**(4), p. 452-61, (1996).
30. H.M. Buettnner, R.N. Pittman, and J.K. Ivins, *A model of neurite extension across regions of nonpermissive substrate: simulations based on experimental measurement of growth cone motility and filopodial dynamics*. Dev Biol, **163**(2), p. 407-22, (1994).
31. H.M. Buettnner, *Computer simulation of nerve growth cone filopodial dynamics for visualization and analysis*. Cell Motil Cytoskeleton, **32**(3), p. 187-204, (1995).
32. H.D. Simpson, D. Mortimer, and G.J. Goodhill, *Theoretical models of neural circuit development*. Curr Top Dev Biol, **87**, p. 1-51, (2009).
33. G.J. Goodhill and H. Baier, *Axon guidance: stretching gradients to the limit*. Neural Comput, **10**(3), p. 521-7, (1998).
34. G.J. Goodhill and J.S. Urbach, *Theoretical analysis of gradient detection by growth cones*. J Neurobiol, **41**(2), p. 230-41, (1999).
35. M.J. Katz and R.J. Lasek, *Early axon patterns of the spinal cord: experiments with a computer*. Dev Biol, **109**(1), p. 140-9, (1985).
36. R. Segev and E. Ben-Jacob, *Generic modeling of chemotactic based self-wiring of neural networks*. Neural Netw, **13**(2), p. 185-99, (2000).
37. J.K. Krottje and A. van Ooyen, *A mathematical framework for modeling axon guidance*. Bull Math Biol, **69**(1), p. 3-31, (2007).
38. Y. Sakumura, Y. Tsukada, N. Yamamoto, and S. Ishii, *A molecular model for axon guidance based on cross talk between rho GTPases*. Biophys J, **89**(2), p. 812-22, (2005).
39. A. Jilkine, A.F. Maree, and L. Edelstein-Keshet, *Mathematical model for spatial segregation of the Rho-family GTPases based on inhibitory crosstalk*. Bull Math Biol, **69**(6), p. 1943-78, (2007).
40. A. Mogilner and B. Rubinstein, *The physics of filopodial protrusion*. Biophys J, **89**(2), p. 782-95, (2005).
41. Padmanabhan, P., and G.J. Goodhill. *Axon growth regulation by a bistable molecular switch*. Proceedings Royal Society B Biological sciences, **285**(1877) (2018).
42. H.G. Hentschel and A. van Ooyen, *Models of axon guidance and bundling during development*. Proc Biol Sci, **266**(1434), p. 2231-8, (1999).
43. G.J. Goodhill, M. Gu, and J.S. Urbach, *Predicting axonal response to molecular gradients with a computational model of filopodial dynamics*. Neural Comput, **16**(11), p. 2221-43, (2004).
44. S. Maskery and T. Shinbrot, *Deterministic and stochastic elements of axonal guidance*. Annu Rev Biomed Eng, **7**, p. 187-221, (2005).

45. Y.E. Pearson, E. Castronovo, T.A. Lindsley, and D.A. Drew, *Mathematical modeling of axonal formation. Part I: Geometry*. Bull Math Biol, **73**(12), p. 2837-64, (2011).
46. T. Betz, D. Lim, and J.A. Kas, *Neuronal growth: a bistable stochastic process*. Phys Rev Lett, **96**(9), p. 098103, (2006).
47. Rizzo, D.J., J.D. White, E. Spedden, M.R. Wiens, D.L. Kaplan, T.J. Atherton, and C. Staii, *Neuronal growth as diffusion in an effective potential*. Physical Review E, 2013. **88**: p. 042707.
48. Beighley, R., E. Spedden, K. Sekeroglu, T. Atherton, M.C. Demirel, and C. Staii, *Neuronal alignment on asymmetric textured surfaces*. Applied Physics Letters, 2012. **101**: p. 143701.
49. Spedden, E., M.R. Wiens, M.C. Demirel, and C. Staii, *Effects of surface asymmetry on neuronal growth*. PLoS One, 2014. **9**(9): p. e106709.
50. Vensi Basso, J.M., I. Yurchenko, M. Simon, D.J. Rizzo, and C. Staii, *Role of geometrical cues in neuronal growth*. Phys Rev E, 2019. **99**(2-1): p. 022408.
51. Yurchenko, I., J.M. Vensi Basso, V.S. Syrotenko, and C. Staii, *Anomalous diffusion for neuronal growth on surfaces with controlled geometries*. PLoS One, 2019. **14**(5): p. e0216181.
52. Basso, J.M.V., I. Yurchenko, M.R. Wiens, and C. Staii, *Neuron dynamics on directional surfaces*. Soft Matter, 2019. **15**: p. 9931-41.
53. Yurchenko, I., M. Farwell, D. D. Brady, and C. Staii, *Neuronal Growth and Formation of Neuron Networks on Directional Surfaces*, Biomimetics, 2021. **6**(2): p. 1-14
54. Sunnerberg, J.P., M. Descoteaux, D. L. Kaplan, and C. Staii, *Axonal growth on surfaces with periodic geometrical patterns*. PLoS One, 2021. **16**(9): p. e0257659.
55. Descoteaux, M., J.P. Sunnerberg, D. D. Brady, and C. Staii, *Feedback-controlled dynamics of neuronal cells on directional surfaces*. Biophysical Journal, 2022. **121**(5), p. 769-781.
56. Spedden, E., J.D. White, E.N. Naumova, D.L. Kaplan, and C. Staii, *Elasticity maps of living neurons measured by combined fluorescence and Atomic Force Microscopy* Biophysical Journal, 2012. **103**: p. 868-877.
57. Spedden, E. and C. Staii, *Neuron biomechanics probed by atomic force microscopy*. International Journal of Molecular Sciences, 2013. **14**: p. 16124-40.
58. Spedden, E., D.L. Kaplan, and C. Staii, *Temperature response of the neuronal cytoskeleton mapped via atomic force and fluorescence microscopy*. Physical Biology, 2013. **10**: p. 056002.
59. Sunnerberg, J.P., P. Moore, E. Spedden, D.L. Kaplan, and C. Staii, *Variations of Elastic Modulus and Cell Volume with Temperature for Cortical Neurons*. Langmuir, 2019. **35**(33): p. 10965-10976.
60. Simon, M., M. Dokukin, V. Kalaparathi, E. Spedden, I. Sokolov, and C. Staii, *Load Rate and Temperature Dependent Mechanical Properties of the Cortical Neuron and Its Pericellular Layer Measured by Atomic Force Microscopy*. Langmuir, 2016. **32**(4): p. 1111-9.
61. Wang, M.D. *Manipulations of single molecules in biology*, Curr. Opin. Biotechnol. 1999. **10**(1): p. 81-86.
62. Sahu, S., L. Herbst, R. Quinn, and J.L. Ross, *Crowder and surface effects on self-organization of microtubules*. Phys. Rev. E, 2021. **103**(6): p. 062408.
63. Bleicher, P. and A. R. Bausch, *Self-organization in reconstituted actin networks by coupling monomer turnover and contractility*. Biophysical Journal, 2022. **121**(3): p. 518A.

64. Swanson, D. and N.S. Wingreen, *Active biopolymers confer fast reorganization kinetics*. Phys. Rev. Lett. **107**(21): p. 218103.
65. Risken, H. *The Fokker-Planck equation: methods of Solutions and Applications*, 2nd edition (Springer, Berlin 1996).
66. Notbohm, J., S. Banerjee, K. J. C. Utuje, B. Gweon, H. Jang, Y. Park, J. Shin, J. P. Butler, J. J. Fredberg, and M. C. Marchetti, *Cellular contraction and polarization drive collective cellular motion*, Biophysical Journal, 2016. **110**: p. 2729-2738.
67. Banerjee S., and M.C. Marchetti, *Substrate rigidity deforms and polarizes active gels*. Europhysics Letters, 2011. **96**: p. 28003.
68. Dokukina I.V., and M.E. Gracheva, *A model of fibroblast motility on substrates with different rigidities*. Biophysical Journal, 2010. **98** p. 2794-2803.
69. Alert, R. and X. Trepat, *Physical Models of collective cell migration*. Annual Review of Condensed Matter Physics, 2020. **11**: p. 77-101.
70. Farhadifar, R., J.C. Roper, B. Aigouy, S. Eaton, and F. Julicher, *The influence of cell mechanics, cell-cell interactions, and proliferation on epithelial packing*. Curr Biol, 2007. **17**(24): p. 2095 -104.
71. Marchetti, M.C., J. F. Joanny, S. Ramaswamy, T.B. Liverpool, J. Prost, M. Rao, and A. Simha, *Hydrodynamics of soft active matter*. Rev Mod Phys, 2013. **85**(3): p. 1143.
72. Nelson, P.C. *Biological physics: Energy, Information, Life*. Student edition, 2020.
73. Zeravcic, Z., V.N. Manoharan, and M.P. Brenner, *Colloquium: Toward living matter with colloidal particles*, Rev. Mod. Phys. 2017. 89: p. 031001.
74. Phillips, R., J. Kondev, J. Theriot, H. G. Garcia, *Physical biology of the cell*, 2nd edition (Garland Science, Taylor and Francis Group, 2013).
75. Zhi, Y. and D. Cox, *Neurodegenerative damage reduces firing coherence in a continuous attractor model of grid cells*, Phys. Rev. E, 2021. **104**(4): p. 044414.
76. Devany J., D.M. Sussman, T. Yamamoto, M.L. Manning, and M.L. Gardel, *Cell cycle-dependent active stress drives epithelia remodeling*. Proc Natl Acad Sci USA, 2021. **118**(10): p. e1917853118.
77. Beniash, E., C.A. Stifler, C-Y. Sun, G.S. Jung, Z. Qin, M.J. Buehler and Pupa U.P.A. Gilbert, *The hidden structure of human enamel*. Nature Communications, 2019. **10**: p.1-13.
78. Cartagena-Rivera, A.X., W-H. Wang, R. L. Geahlen, and A. Raman, *Fast, multi-frequency, and quantitative nanomechanical mapping of live cells using the atomic force microscope*, Nature Scientific Reports, 2015. **5**, p. 11692.
79. Moore, J.M., T. N. Thompson, M. A. Glaser, and M.D. Betterton, *Collective motion of driven semiflexible filaments tuned by soft repulsion and stiffness*, (2020). Soft Matter **16**: p. 9436-9442.
80. Kumarasinghe U.H., M. Farwell, and C. Staii, *Combined traction force-atomic force microscopy measurements of neurons*, *submitted 2022*.
81. Kundu, A., L. Micholt, S. Friedrich, D. R. Rand, C. Bartic, D. Braeken, and A. Levchenko, *Superimposed topographic and chemical cues synergistically guide neurite outgrowth*. Lab on a chip, 2013. **13**(15): p. 3070-3081.
82. Wang, N., J.D. Tytell, and D.E. Ingber, *Mechanotransduction at a distance: mechanically coupling the extracellular matrix with the nucleus*. Nat Rev Mol Cell Biol, 2009. **10**(1): p. 75-82.

83. Riveline, D., E. Zamir, N.Q. Balaban, U.S. Schwarz, T. Ishizaki, S. Narumiya, Z. Kam, B. Geiger, and A.D. Bershadsky, *Focal contacts as mechanosensors: externally applied local mechanical force induces growth of focal contacts by an mDia1-dependent and ROCK-independent mechanism*. J. Cell. Biol. 2001. **153**: p. 1175-1186.